Local Microstructure Characterization of Rare Earth-Doped PMMA with Low-Ion Content by Fluorescence EXAFS

Hui Zhao,[1,2] Jun Hu,[2] Qijin Zhang,[2] Jun Bao,[3] Wenhan Liu,[4] Chen Gao,[3] Yanhua Luo[2]

[1]*Structure Research Laboratory, University of Science and Technology of China, Hefei, Anhui, People's Republic of China*
[2]*Department of Polymer Science and Engineering, University of Science and Technology of China, Hefei, Anhui, People's Republic of China*
[3]*National Synchrotron Radiation Laboratory,University of Science and Technology of China, Hefei, Anhui, People's Republic of China*
[4]*Department of Physics, University of Science and Technology of China, Hefei, Anhui, People's Republic of China*

Received 20 December 2004; accepted 5 July 2005
DOI 10.1002/app.23498
Published online in Wiley InterScience (www.interscience.wiley.com).

ABSTRACT: Fluorescence-extended X-ray absorption fine structure (EXAFS), and emission spectrum and excitation spectrum (ESES) were used to characterize the local structure of rare earth-doped poly(methyl methacrylate)s (Re-PMMAs) with ion concentration of 600–1000 ppm. Fluorescence EXAFS shows that the chemical state of Sm in Sm-PMMA is the same as that in Sm_2O_3 and samarium octanoate (SOA), while that of Eu in Eu-PMMA is different from that in Eu_2O_3 and europium octanoate. ESES also proves the concomitance of Eu^{2+} with Eu^{3+} ions in Eu-PMMA. And, the almost identical peak positions of Eu L_3 edge at ~6976.7 eV in fluorescence EXAFS of Eu-PMMA with various Eu content suggests the proportions of Eu^{2+} to Eu^{3+} are the same in these samples. The simulation of fluorescence EXAFS shows that the first-shell coordination number of Sm^{3+} in Sm-PMMA is 9.12, and the average first-shell distance around Sm^{3+} in Sm-PMMA is 2.43 Å.

Key words: fluorescence; X-ray; microstructure; metal–polymer complexes

INTRODUCTION

Polymer optical fibers (POFs) have received much interest in the past decades because they can be made with larger core diameter, which results in POF being one of the promising candidates of fiber to the desktop.[1] Rare earth-doped POF with low-ion content can be used as functional materials for devices of POF lasers and POF amplifiers, and some works have been reported on these interesting applications[2–4] On the other hand, to optimize the emission properties of this class of materials, there are still a few fundamental issues that need to be addressed and eventually resolved. One of such issues is how the mechanism of optical processes is influenced by the local microstructure of luminescent materials. Through understanding and controlling the microscopic order, it is possible to modify and improve the macroscopic emission characteristics.[5]

Recently, detailed relationship between mechanism of photoluminescence and characteristic structure of rare earth complexes has also attracted much attention, such as narrow bandwidth of luminescence from europium complex,[6] and polarized europium emission.[7] In the latter work, it has been found that the emission of the material is dependent on microstructure of rare earth complex with concentration of 30 wt %, which is the result of interaction between the complex and polymer chains under tensile drawing. However, there is little work on directly characterization of local microstructure of rare earth-doped polymer, especially for samples with low-ion content.

EXAFS can access the information on the local microstructure of metal ions-doped polymers,[8,9] and is becoming one of the methods to characterize the structure and microstructure of ionomers,[10,11] especially those with nanometer-sized aggregates.[12] The interpretation of EXAFS is usually based on the single-electron single scattering theory,[13] from which oscillations in the X-ray absorption coefficient above the X-ray absorption edge can be related to the local structure around the atoms. EXAFS signal can be measured in two ways: direct measurement of absorption coefficient by detecting the transmitted X-ray intensity or indirect measurement by detecting the sequential events after the X-ray absorption, such as Auger elec-

Correspondence to: Q. Zhang (zqjm@usthichaf0dbchaf17c.edu.cn).

Contract grant sponsor: National Natural Science Foundation of China; contract grant number: 50025309 and 90201016.

TABLE I
Composition of Re-PMMA Samples

Sample	Rare earth element	Concentration of rare earth elements (ppm)
Eu600	Eu	600
Eu800	Eu	800
Eu1000	Eu	1,000
Sm800	Sm	800

tron or fluorescent radiation. For samples with low rare earth content, fluorescence EXAFS is an efficient method, but has not been used in study on the local microstructure of rare earth-doped polymer. It is well-known that europium-doped polymer has a relative strong emission at about 613 nm,[6,7] which can be used as a suitable sample for study by fluorescence of EXAFS. In this work, europium and samarium octanoates-doped poly(methyl methacrylate) (Re-PMMA) with low concentration (several hundreds ppm of ion) was synthesized, and the local microstructure is characterized by fluorescence EXAFS and compared with corresponding small molecules.

EXPERIMENTAL

Materials

Rare earth octanoates (ROAs) were synthesized by the method outlined earlier.[14] Designed amount of ROA was dissolved in acrylic acid and then added to a solution containing methyl methacrylate (MMA), azobisisobutyronitrile(AIBN), dodecyl mercaptan, and bromobenzene (BB). The mixture was prepolymerized at 80°C for 1 h, and then poured into a tube. The tube was placed at 70°C until the solidification was completed. After that, the tube was placed at about 100°C in vacuum for 2 h. In this way, rare earth-doped poly(methyl methacrylate) (Re-PMMA) rods were synthesized. Table I lists the compositions of the Re-PMMA samples used in this work.

For samples used in measurement of fluorescence EXAFS, rare earth oxides and octanoates were diluted by SiO_2 to 1% (wt), and Re-PMMA were obtained by cutting the polymer rods into $1 \times 10 \times 80$ mm^3 chips.

Fluorescence EXAFS

Fluorescence EXAFS experiments were carried out on the EXAFS station at the Beijing synchrotron radiation facility (BSRF 4W1B) operated at 2.2 GeV and an average stored current of 80 mA. A Si(111) double-crystal monochromator was used. The scanning energy range was from 200 eV below to 650 eV above the Eu or Sm L_3-edge. From 200 to 20 eV below the edge, 5 eV steps were used: 1 eV steps were used from 20 eV below to 50 eV above the edge. From 50 to 300 eV above the edge, 2 eV steps were used. 3 eV steps were used from 300 to 420 eV above the edge. 4 eV steps were used above 420 eV above the edge. During the measurement, 3-mm Mn high-pass filter was used.

Emission spectrum and excitation spectrum

The emission spectrum and excitation spectrum of Eu800 and Eu1000 were measured with a fluorescence spectrometer (970CRT). The sample was excited by 335 nm light of Xe lamp, and the emitting fluorescence intensity was received by photomultiplier through monochromater. The spectra were obtained by filtering excitation light with a 420 nm high-pass filter. Both of Eu800 and Eu1000 samples for the measurement were 1-mm-thick chips.

RESULTS AND DISCUSSION

It has been well-known that EXAFS is one effective method to detect the local structure around rare earth ions,[8,9] in which EXAFS is obtained by directly measuring the transmitted X-ray intensity. When the ion content is low, X-ray intensity is not changing much before and after transmission, which results in a small ratio of signal to noise, and EXAFS cannot be obtained. When the rare earth concentration in samples is very low, such as several hundreds ppm, fluorescence EXAFS should be adopted. In fluorescence EXAFS, EXAFS signal is indirectly obtained by detecting the fluorescent radiation after the X-ray absorption. The ratio of signal to noise is large enough to give information about local microstructure.

PMMA doped with samarium octanoate

After linear extrapolation and subtraction of the pre-edge bulk-absorption contribution using the Victoreen formula and removal of a smooth postedge background with cubic splines, the data were normalized and converted to wave factor (k) space, and the E_0 value was taken at the maximum of the first derivative of the spectrum. The resulting oscillations were weighed with k^2 factor and Fourier transformed to radial distribution functions. The radial structure function (RSF) is similar to a radical distribution function, because peaks in the RSF corresponded to distinct coordination shells, but the location of the peaks are shifted from the real distance; hence, F will be used as a subscript to distinguish this distance from the actual interatomic distance R. Reduction procedures for all date sets were identical to enable direct comparison of results.

Figure 1 shows the fluorescence EXAFS results for samples of samarium oxide(Sm_2O_3), samarium octanoate(SOA), and samarium octanoate-doped PMMA(SOA-PMMA), respectively. The sharp rise in μ at 6722.9 eV is

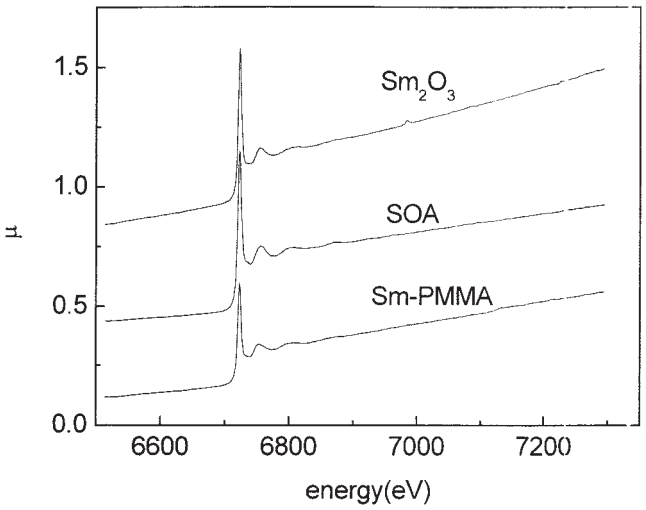

Figure 1 Fluorescence EXAFS of Sm_2O_3, SOA, and Sm-PMMA at a temperature of 298 K. The sharp rise in μ at 6722.9 eV is the L_3 edge and the modulation in μ above the edge is the EXAFS.

the L_3 edge of Sm, and the modulation in μ above the edge is the EXAFS. In 1970, Agawall et al. found that the position of edge of metal in EXAFS depend on the chemical state of the metal ion.[15] From the result in Figure 1, it can be seen that there is no change in the oxidation state of Sm^{3+} in different matrices.

As the chemical state of Sm^{3+} in the samples is of stability as described earlier, local microstructure of Sm-containing samples can be obtained by further analysis of their fluorescence EXAFS. Figure 2 gives the RSF curves of SOA and Sm800. It is known that the locations of the first-shell coordination peak center R_F is related to the coordination distance. In Figure 2, the first-shell peak of RSF of Sm-PMMA is centered near R_F = 1.8 Å, while that of SOA is centered near R_F = 1.9 Å. It is speculated that the average first-shell coordination distance of Sm-PMMA would be smaller than that of SOA.

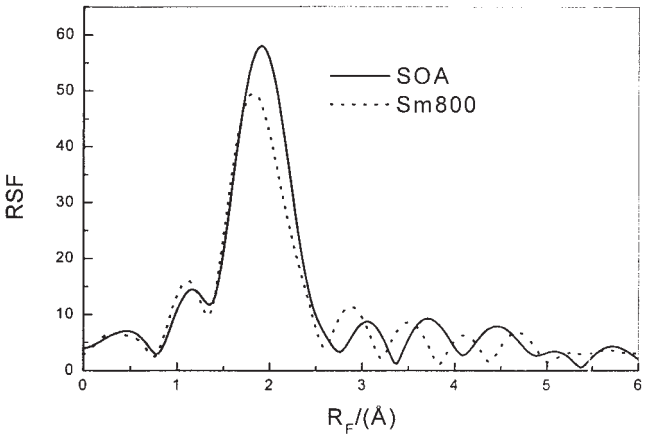

Figure 2 RSF curves of SOA (solid line) and Sm800 (dotted line).

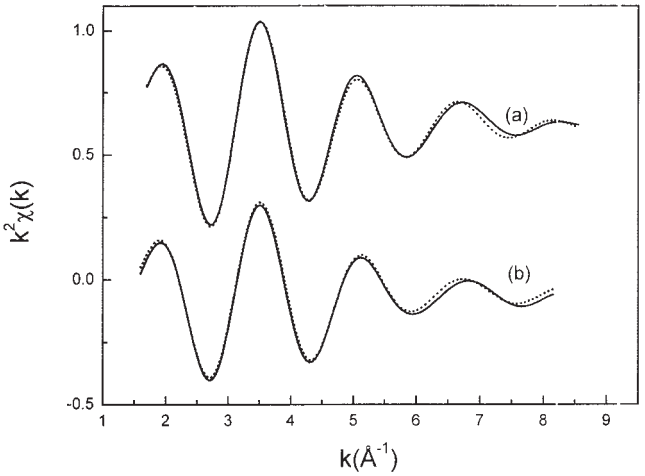

Figure 3 Fourier-filtered first-shell EXAFS oscillation (solid line) and nonlinear least-squares fits (dotted line) for (a) SOA and (b) Sm-PMMA.

The RSFs of the two samarium samples were Fourier-filtered using the Hanning windows to isolate first-shell contributions as amplitude and phase functions, as shown by solid lines in Figure 3. In this work, we used the least squares curve fitting based on Marquardt's scheme for iterative estimation of nonlinear least squares parameters via a compromise combination of gradient and Taylor series method 34 to fit the Fourier-filtered EXAFS oscillations in a k space.[16] Dotted lines in Figure 3 show the fitted lines. It can be seen from Figure 3 that good fits were obtained for two samples, and the agreement factor (R) is about 0.01 in the calculations as shown in Table II. The numerical results are also summarized in Table II, which shows that first-shell coordination number of SOA and Sm-PMMA are 9.35 and 9.12, respectively, and the first-shell distance around Sm^{3+} for SOA and Sm-PMMA are 2.46 and 2.43 Å, respectively. It is obvious that the first-shell distance of Sm-PMMA is slightly smaller than that of SOA.

It has been known that there are two kinds of chemical bonds in complexes of rare earth ions, bridging and chelating, as shown as in Figure 4(a). By bridging bonds, one carbonyl group links two ions, and then a net structure will be formed, which cannot be dissolved in MMA. Before the polymerization for making

TABLE II
Structural Parameters of Sm Samples Obtained from EXAFS Data

	SOA	Sm-PMMA
R (Å)	2.46 ± 0.01	2.43 ± 0.01
N	9.35 ± 0.9	9.12 ± 0.9
σ^2	0.0085	0.012
R-factor	0.01	0.009

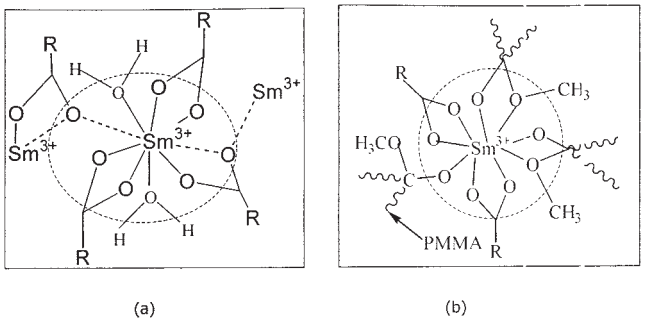

Figure 4 Schematic diagram of bridging bond (dashed line) and chelating bond (solid line) for (a) small molecular rare earth complexes and (b) rare earth-doped polymer. The structure presented as circles (dashed lines) are the local structures.

Sm-PMMA, the structure should be broken by adding stronger acids, such as acrylic acid, or should be eliminated by purification.[17] Two methods have decreased the content of the bridging structure in SOA, which results in dissolution of SOA in MMA. On the other hand, it is known that the bond length of bridging bond is longer than that of chelating bond. For example,[18] the average length of chelating Sm—O bond is 2.484 Å, and the average length of bridging Sm—O bond is 2.505 Å, which indicates that eliminating of bridging Sm—O bonds will decrease the overall average Sm—O bond length. It has been also observed that there is 0.02 Å difference for the first shell of different Eu-containing compounds.[19] From Table II, it can be found that there is a decrease in average length of Sm—O bonds, from 2.46 to 2.43 Å. There is no change in the coordination number for SOA and Sm-PMMA as shown in Table II. Assuming the bridging bond in SOA is substituted with chelating bond in Sm-PMMA and the average bond length in SOA is 2.46 Å, it can be obtained by simple calculation that the average bond length in Sm-PMMA is 2.44 Å, which is identical with the observed value of the first-shell coordinate distance in experiment within error of ±0.01 Å. The schematic diagram of the local structure of Sm-PMMA is shown in Figure 4(b), in which the bridging bonds were substituted with chelating bonds.

From Figure 4(b), it can be seen that there is no bridging bonds in the local structure. That means, each ion is enveloped by polymer chains and there is no ion aggregates in the samples.

PMMA doped with europium octanoate

Different from Sm-containing samples, in fluorescence EXAFS μ_r vs E curves of Eu_2O_3, europium octanoate (EOA), Eu600, Eu800, and Eu1000 shown in Figure 5, the positions of L_3 edge of Eu^{3+} for each sample are located at 6977.3, 6975.6, 6976.7, 6976.7, and 6976.7 eV, respectively. One obvious fact is that L_3 edge of Eu^{3+} for Eu_2O_3, EOA, and polymer samples are different, but it

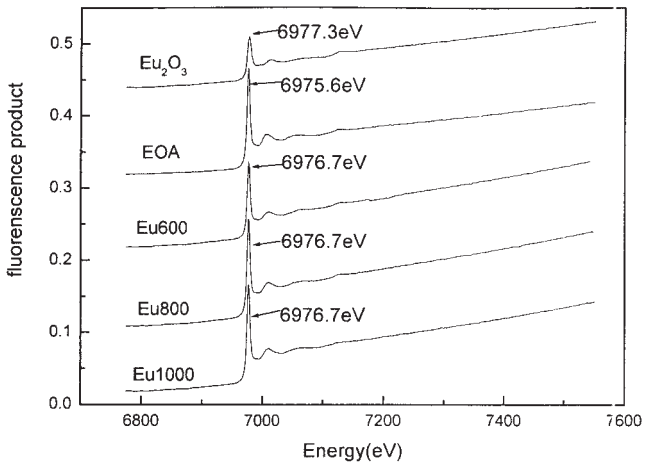

Figure 5 Fluorescence EXAFS μ_r vs E curves of Eu_2O_3, EOA Eu600, Eu800, and Eu1000. The sharp rise in μ near 6980 eV is the L_3, and the modulation in the edge is the EXAFS.

keeps unchanging in polymer samples with different Eu^{3+} content. As mentioned earlier, the position of edge of metal in EXAFS depends on the chemical state of the metal ion.[15] This result shows that there is a change in chemical state of Eu^{3+} in different samples, other than in the same polymer matrices.

The configuration instability was observed in some Eu compounds, which results from valence fluctuations between two (energetically) closely spaced, localized $4f^n$ configurations,[20] and the position of L_3 edge of Eu^{2+} is lower than that of Eu^{3+} [21]. Hence, it can be speculated that the result in Figure 5 be caused by coexisting both of Eu^{3+} and Eu^{2+} in the samples.

On the other hand, in the emission spectrum and excitation spectrum, it was experimentally found that the Eu^{2+} ions are concomitant with Eu^{3+} ions in the Eu-doped PMMA. The measured emission spectra, which were excited by 335 nm light, ranging from 420 to 670 nm, were normalized with Origin software and shown in Figure 6. In Figure 6, three peaks can be

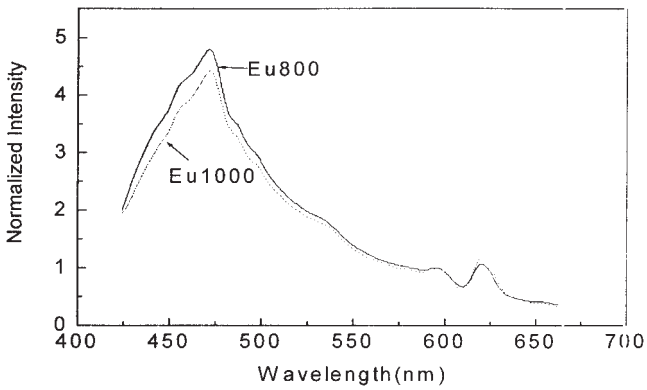

Figure 6 Changes of the relative fluorescence intensity with wavelength for Eu^{3+}-doped PMMA samples of different doped concentration excited by light at 335 nm.

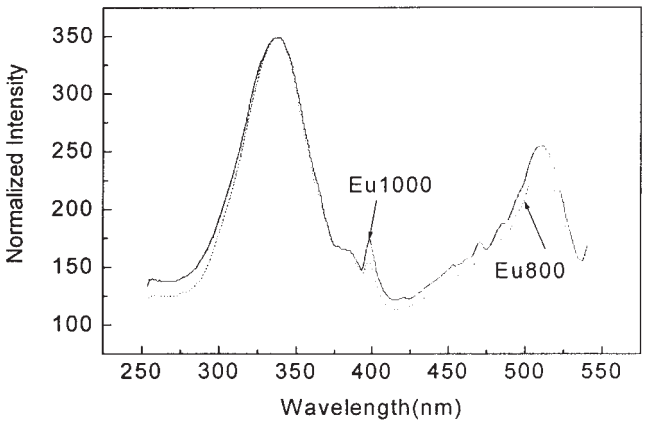

Figure 7 Excitation spectra of Eu^{3+}-doped PMMA samples of different doped concentration corresponding to 616 nm fluorescence.

observed: the broad band at 470 nm is caused by the nonradiative relaxation of the excited electron to the lowest energy level of the $4f^6 5d$ configuration and radiative transition into the ground $^8S_{7/2}$ level of the Eu^{2+} ions; the 593.7 nm peak caused by $^5D_0 \rightarrow {}^7F_1$ transition of Eu^{3+} ions and the 618 nm peak caused by $^5D_0 \rightarrow {}^7F_2$ transition of Eu^{3+} ions. Among the 593.7 nm and 618 nm peaks, the $^5D_0 \rightarrow {}^7F_1$ transition is magnetic dipole transition and its intensity hardly varies with the crystal-field strength acting on Eu^{3+} ions, and the $^5D_0 \rightarrow {}^7F_2$ transition is an electric dipole transition and its intensity is sensitive to chemical bonds in the vicinity of Eu^{3+} ions. So, both spectra lines in Figure 6 are normalized to the peak at 593 nm. The appearance of these three peaks and the broadness of the first peak indicate the coexistence of Eu^{2+} and Eu^{3+} ions. On the other hand, the normalized relative excitation spectrum of $^5D_0 \rightarrow {}^7F_2$ transition of Eu^{3+}(616 nm) was obtained (Fig. 7) by filtering excitation light with a 580 nm high-pass filter. From Figure 7, three obvious exciting peaks are seen. The broad-bond excitation around 335 nm indicates the possibility of Eu^{2+} and Eu^{3+} ions' coexistence. It is worthy to note that, although there are both Eu^{2+} and Eu^{3+} in the Eu complexes, the positions of Eu L_3 edge in Eu600 (at 6976.6 eV), Eu800 (at 6976.7 eV), and Eu1000 (at 6976.9 eV) are almost identical, which indicates the proportion of Eu^{3+} and Eu^{2+} is the same in the three Eu-doped PMMA samples, but for Eu_2O_3, EOA, and polymer samples, the positions of Eu L_3 edge is different, showing the proportion of Eu^{3+} and Eu^{2+} is different in the three samples.

CONCLUSIONS

From study on fluorescence EXAFS of rare earth-doped PMMA with low-ion content, it has been found that the chemical state of Sm in Sm-PMMA is the same as Sm_2O_3 and SOA, while the situation is different in Eu-containing samples. By the analysis of fluorescence EXAFS and ESES, it is realized that it occurred in the concomitance of Eu^{2+} and Eu^{3+} ions in Eu-PMMA with the almost same proportions. Results from fluorescence EXAFS also shows that the first-shell coordination number and distance of Sm—O in Sm-PMMA are 9.12 and 2.43 Å, respectively. On the basis of this data, a simple model is given for the local structure of rare earth-doped PMMA with low-ion content.

The authors thank Prof. T.D. Hu and Y.L. Xie of Beijing Synchortron Radiation Facility for their assistance on the XAFS measurement. We also appreciate the advices from Prof. S.Q. Wei of National Synchrotron Radiation Laboratory on data processing.

References

1. Kaino, T. In Polymers for Lightwave and integrated Optics, Hornak, L., Ed.; Marcel Dekker: New York, 1992; p 1.
2. Zhang, Q. J; Ming, H.; Zhai, Y. J. J Appl Polym Sci 1996, 62, 887.
3. Kobayashi, T.; Nakatsuka, S.; Iwafuji, T.; Kuriki, K.; Imai, N.; Nakamoto, T.; Claude, C. D.; Sasaki, K.; Koike, Y.; Okamoto, Y. Appl Phys Lett 1997, 71, 2421.
4. Koeppen, C.; Yamada, S.; Jiang, G.; Garito, A. F. J Opt Soc Am B 1997, 14, 155.
5. Kohler, A.; Wilson, J. S.; Friend, R. H. Adv Mater 2002, 14, 701.
6. McGehee, M. D.; Bergstedt, T.; Zhang, C.; Saab, A. P.; O'Regan, M. B.; Bazan, G. C.; Srdanov, V. I.; Heeger, A. J Adv Mater 1999, 11, 1349.
7. Yang, C. Y.; Srdanov, V.; Robinson, M. R.; Bazan, G. C.; Heeger, A. J Adv Mater 2002, 14, 980.
8. Grady, B. P.; Moore, R. B. Macromolecules 1996, 29, 1685.
9. Chaboy, J.; Castro, C. J Non-Cryst Solids 1997, 212, 11.
10. Sobczak, J. W.; Sobczak, E.; Lesiak, B.; Palczewska, W.; Kosinski, A. J Alloys Compd 1999, 286, 98.
11. Vidal, P. L.; Divisia-Blohorn, B.; Bidan, G.; Hazemann, J. L.; Kern, J. M.; Sauvage, J. P. Chem Eur J 2000, 6, 1663.
12. Farrell, K. V.; Grady, B. P. Macromolecules 2000, 33, 7122.
13. Teo, B. K. EXAFS: Basic Principles and Data Analysis; New York: Springer-Verlag, 1986.
14. Xu, W. Y.; Wang, Y. S.; Zheng, D. G.; Xia, S. L. J Macromol Sci Chem 1998, A25, 1397.
15. Agarwal, B. K.; Verma, L. P. J Phys C: Solid State Phys 1970, 3, 535.
16. Marquardt, D. W. J Soc Indust Appl Math 1963, 11, 431.
17. Zhang, Q. J; Liu, W.; Dai, P. Polymer 1998, 39, 3787.
18. Arias, J. L.; Cabrera, A.; Sharma, P.; Rosas, N.; Garcia, J. L.; Hernandez, S. Inorganica Chimica Acta 2000, 310, 261.
19. Tao, Y.; Zhao, G. W.; Ju, X.; Shao, X. G.; Zhang, W. P.; Xia, S. D. Mater Lett 1996, 28, 137.
20. Kalvius, G. M. J Alloys Compd 1995, 223, 242.
21. Liang, H. B.; Su, Q.; Tao, Y.; Hu, T. D.; Liu, T.; Shulin, S. L. E. J Phys Chem Solids 2002, 63, 719.